ARMY RESEARCH LABORATORY

Shock Response of a Heavy Tungsten Alloy

by Dattatraya P. Dandekar and William J. Weisgerber

ARL-RP-9 October 2000

A reprint from the *International Journal of Plasticity*, vol. 15, pp. 1291–1309, August 1999.

The findings in this report are not to be construed as an official Department of the Army position unless so designated by other authorized documents.

Citation of manufacturer's or trade names does not constitute an official endorsement or approval of the use thereof.

Destroy this report when it is no longer needed. Do not return it to the originator.

Army Research Laboratory
Aberdeen Proving Ground, MD 21005-5066

ARL-RP-9 October 2000

Shock Response of a Heavy Tungsten Alloy

Dattatraya P. Dandekar and William J. Weisgerber
Weapons and Materials Research Directorate, ARL

A reprint from the *International Journal of Plasticity*, vol. 15, pp. 1291–1309, August 1999.

Abstract

This article describes the results of shock wave experiments performed on a heavy tungsten alloy containing W, Ni, and Fe in the ratio of 92.85:4.9:2.25 by weight. These experiments provide information about the shear strength under compression and tensile strength, as measured by the spall threshold, of this alloy to 24 GPa. The results of these experiments show that: (i) the magnitude of its Hugoniot elastic limit (HEL) is 2.76 ± 0.26 GPa; (ii) this alloy deforms plastically above its HEL and thus retains its shear strength to 24 GPa; (iii) the spall strength of the alloy is found to be 1.9 ± 0.4 GPa and is independent of the impact stress and duration of the shock compression pulse; and (iv) the tensile impedance of the alloy, determined from a new experiment designed to measure this impedance, is 68 ± 10 Gg/m^2 s.

PERGAMON

International Journal of Plasticity 15 (1999) 1291–1309

INTERNATIONAL JOURNAL OF Plasticity

Shock response of a heavy tungsten alloy

Dattatraya P. Dandekar*, William J. Weisgerber

US Army Research Laboratory, Aberdeen Proving Ground, Maryland, 21005-5069, USA

Received in final revised form 4 August 1999

Abstract

This article describes the results of shock wave experiments performed on a heavy tungsten alloy containing W, Ni, and Fe in the ratio of 92.85:4.9:2.25 by weight. These experiments provide information about the shear strength under compression and tensile strength, as measured by the spall threshold, of this alloy to 24 GPa. The results of these experiments show that: (i) the magnitude of its Hugoniot elastic limit (HEL) is 2.76 ± 0.26 GPa; (ii) this alloy deforms plastically above its HEL and thus retains its shear strength to 24 GPa; (iii) the spall strength of the alloy is found to be 1.9 ± 0.4 GPa and is independent of the impact stress and duration of the shock compression pulse; and (iv) the tensile impedance of the alloy, determined from a new experiment designed to measure this impedance, is 68 ± 10 Gg/m^2 s.

Keywords: Shock response; Heavy tungsten alloys

1. Introduction

Heavy tungsten alloy is a composite material. It consists of two phases, namely, a predominantly tungsten phase (in body-centered-cubic phase) and a matrix phase composed of W, Ni, and Fe (in face-centered-cubic phase). Tungsten is alloyed to improve its ductility under compression and tension in comparison to that of pure polycrystalline tungsten. The improvement in ductility under shock compression is indicated by the magnitude of shear stress sustained. Under tension it is measured by the magnitude of spall threshold. This work was undertaken to determine both of these properties of a tungsten alloy containing W, Ni, and Fe in the ratio of 92.85:4.9:2.25 by weight under shock loading condition, compared with those of pure polycrystalline tungsten (Dandekar, 1976; Asay et al., 1980; Zurek and Gray III, 1991), and other heavy tungsten alloys, annealed 93W (Baoping et al., 1994), 90 W-7 Ni-3 Fe (Hauver,

* Corresponding author. Tel.: +1-410-306-0801; fax: +1-410-306-0783.
E-mail address: ddandek@arl.mil (D.P. Dandekar).

0749-6419/99/$ - see front matter
PII: S0749-6419(99)00041-8

1980; Zurek and Gray III, 1991; Chang and Choi, 1998) and Kennertium Grade W-2 consisting of tungsten, nickel, iron, copper, and cobalt (Gaeta and Dandekar, 1988).

2. Material

Tungsten alloy used in the present work is manufactured by Teledyne. The nominal composition of this material, provided by the vendor, is given in Table 1. The processing history of this alloy, as reported by its manufacturer, is as follows. An elemental mixture of tungsten, nickel, and iron powders was isostatically pressed at 207 MPa and room temperature. This pressed material was then sintered in a molybdenum wound furnace at 1793 K in a dry hydrogen atmosphere to prevent oxidation of the elemental powder surfaces. The sintered material was then vacuum-annealed at 1273 K for 10 h to remove the adsorbed hydrogen. The annealed material was subsequently heated in an inert gas atmosphere to 1373 K and kept at this temperature for 1 h before being water-quenched. The quenched material was then machined into a bar shape and swaged to a 17% reduction in area. The microstructure of this material consists of nearly equiaxed tungsten grains dispersed in (surrounded by) the matrix phase consisting of tungsten, nickel and, iron. There is no difference in the microstructure of this alloy when viewed in the axial and radial direction of the as received bar. This indicates that the process of swaging did not deform the tungsten grain preferentially (Fig. 1). The nominal composition (in weight percentage) of the matrix phase is reported to be W (25), Ni (50), and Fe (25) (Ekbom, 1981; Hofmann and Petzow, 1984; O'Donnell and Woodward, 1990). The grain size of tungsten varies between 25 and 28 μm (Weerasooriya and Moy, 1998).

Table 1
Nominal composition and properties of polycrystalline tungsten (W), 93W, 93W(A), (90 W), and W-2

Item	Units	W Lowrie and Gonas (1965)	93W	93W (A) Baoping et al. (1994)	90 W Hauver (1980)	90 W Chang and Choi (1998)	W-2 Gaeta and Dandekar (1988)
Composition	Weight percentage						
Tungsten		99.99	92.85	93	90	90	96.96–97.44
Nickel			4.9	4	7	7	1.35–1.55
Iron			2.25	3	3	3	0.65–0.79
Copper							0.48–0.58
Cobalt							0.08–0.12
Swaged	Percentage	Unknown	17	Annealed	25	24	Unswaged
Density	Gg/m^3	19.257 ± 0.004	17.75 ± 0.05	17.6	17.068 ± 0.045	17.1	18.51 ± 0.03
Elastic wave velocity	km/s						
Longitudinal		5.216 ± 0.005	5.18 ± 0.05	not reported	5.08	5.11	5.18 ± 0.02
Shear		2.883 ± 0.001	2.81 ± 0.04	not reported	2.72	–	2.84 ± 0.02
Poisson's ratio		0.280 ± 0.001	0.292 ± 0.019	not reported	0.298	–	0.285 ± 0.012

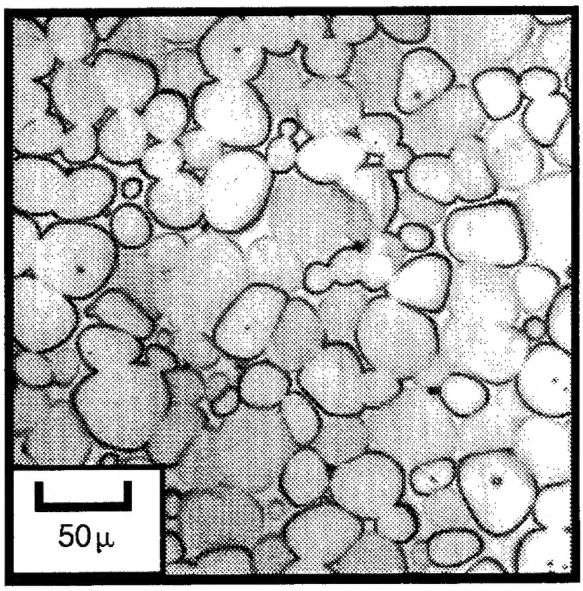

Fig. 1. Microstructure of 93W–5Ni-2 Fe.

The measured density of the tungsten alloy, hereafter referred to as 93W, is 17.75 ± 0.05 Mg/m^3. The density of vacuum annealed tungsten alloy [93W(A)] with a similar composition is reported to be 17.6 Mg/m^3 (Baoping et al., 1994). The values of longitudinal and shear elastic wave velocities in 93W, measured by an ultrasonic wave velocity technique, are 5.18 ± 0.05 and 2.81 ± 0.04 km/s, respectively. These values of the elastic wave velocities are not significantly different from those in polycrystalline tungsten and W-2 alloy but the values of their elastic constants differ due to the differences in their densities (Table 1). The density of the matrix phase is reported to be 9.2 Mg/m^3. The values of longitudinal and shear elastic wave velocities, and Poisson's ratio for this phase are 6.03 and 3.2, and 0.29 km/s, respectively (Zhou et al., 1992).

3. Experiments

Plane shock wave experiments were performed on a 10 cm diameter single-stage gas gun facility at the US Army Research Laboratory. Plane shock wave in a material is generated by impacting it with a flat-faced projectile propelled by pressurized helium gas. Two types of experiments were conducted on 93W. These were transmission experiments with or without a window material bonded behind a specimen of 93W and direct impact experiments. The transmission experiments provided information about the nature of wave propagation and spall threshold (i.e. tensile strength of 93W). The direct impact experiments provided information about the shock compressed state and release therefrom in this alloy without requiring any information about its physical or mechanical properties. Asay et al. (1980), and Gaeta and Dandekar (1988) gave details of the conventional transmission experiments and direct impact experiments.

During this investigation, a new experiment was designed to obtain the effective tensile impedance of a material. The magnitude of tensile impedance of the material is needed to calculate the spall threshold (tensile strength) from the pull-back particle velocity recorded in the shock wave profile. A generally accepted practice assumes its value based on the observed deformation behavior of the material under shock compression and release, which is then used in the calculation of the spall threshold of the material. Dandekar (1996), and Dandekar and Weisgerber (1998) describe the design of this new experiment. The new experiment is described here with the help of Figs. 2 and 3. Briefly, a pair of simultaneous spall experiments is conducted on 93W, in which the impactees/targets and the impactors are the same material (Fig. 2). The targets are thicker than the impactors. In one of these experiments, particle velocity is monitored at the free surface of the material [Fig. 2(a)], whereas, in the companion experiment, particle velocity is monitored at the material–window interface [Fig. 2(b)]. The window material is transparent and its impedance is much lower than the target material. Further it is assumed that shock, release, and reshock response of the window material is fully known. The window material used in the present work is PMMA. In addition the design of the experiment requires that the tensile stress generated in both stationary targets exceed the spall threshold of the target material. The associated $X-t$ diagram and stress(σ)-particle velocity (u) diagrams for both configurations of the experiment are shown in Figs. 2(c) and 3, respectively. Fig. 3(a) and 3(b) shows, respectively, $\sigma - u$ diagrams for the cases when the target material spalls and when it does not. In the following description of the chronological events taking place in the target and the impactor it is assumed that the target spalls.

As a result of an impact with a velocity of u_0, compressive stress waves of magnitude σ_1 [shown as state 1 in Fig. 2(c)] are generated in both the impactor and the target and they propagate away from the respective impact surfaces. These two

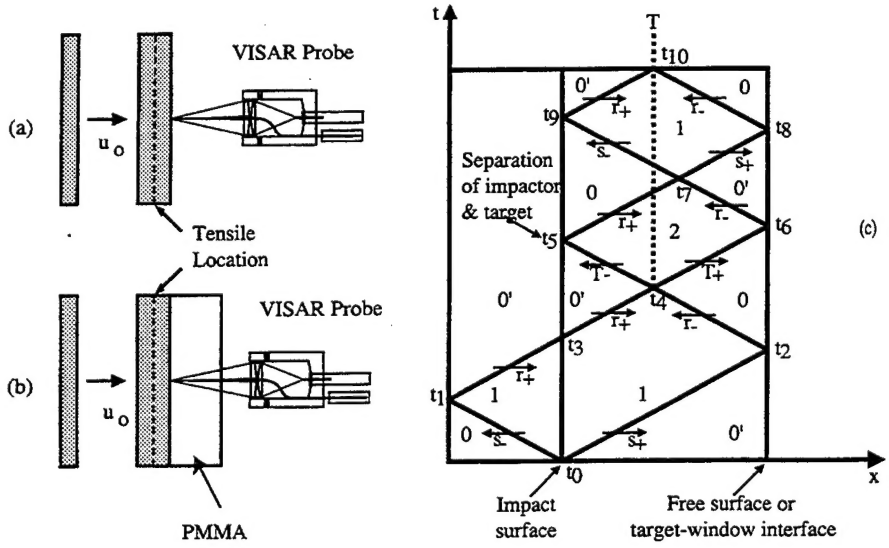

Fig. 2. Configuration of shock wave experiment to measure tensile impedance (a) and (b), and (c) associated x-t diagram.

compressive/shock waves are denoted by s_- and s_+, respectively in Fig. 2(c) and are represented by the segments $u_0 - \sigma_1$ and $0 - \sigma_1$, respectively in Fig. 3(a). Subsequent reflections of these shock waves at the free surface of the impactor at time t_1 and at the free surface of the target or at target–window interface at time t_2 result in propagation of release waves traveling back toward the impact surfaces. These release waves are denoted by r_+ and r_-, respectively in Fig. 2 (c). The release wave r_+ is represented by segment $\sigma_1 - u_{2'}$ in Fig. 3(a). The release wave r_- corresponding to configurations Fig. 2 (a) and (b) are represented by $\sigma_1 - u_2$ and $\sigma_1 - \sigma_3$, respectively in Fig. 3(a). The release states attained in the impactors are zero stress and particle velocity of magnitude $u_{2'}$. The release state attained at the free-surface of the target

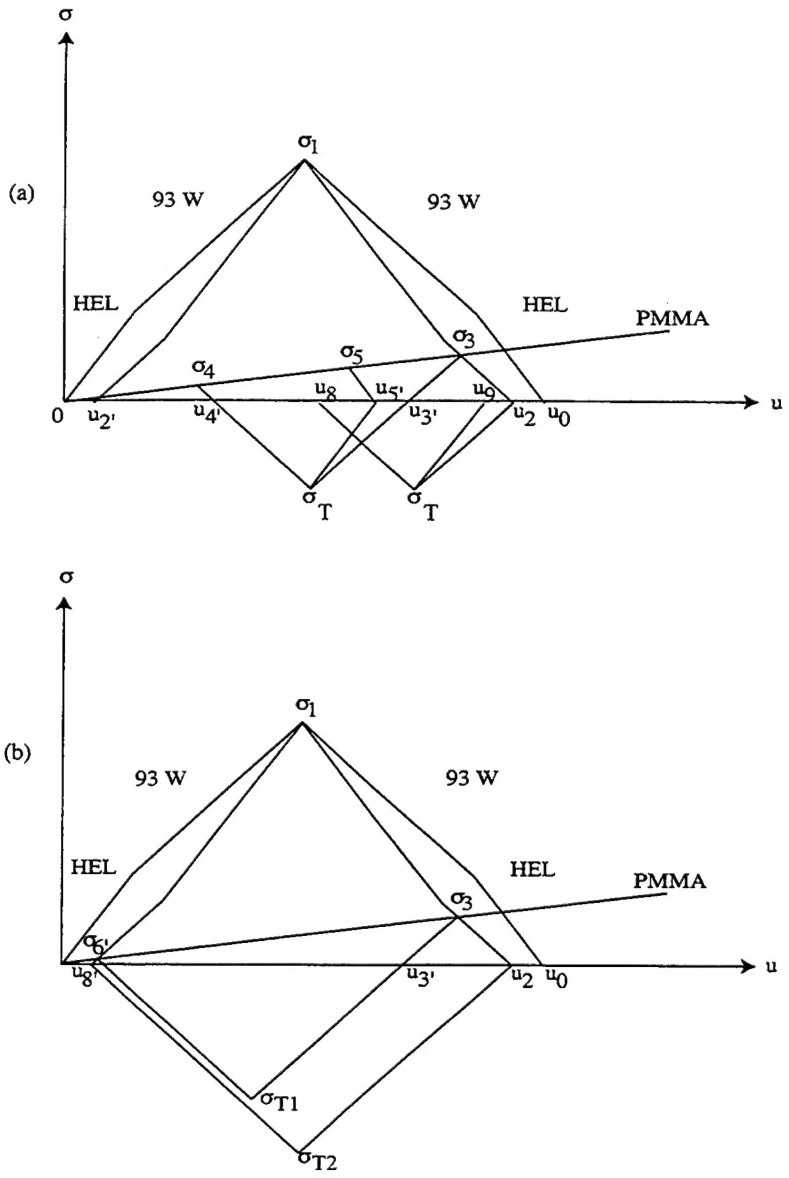

Fig. 3. Stress–particle velocity diagram, (a) if material spalls and (b) if material remains intact under tension.

is zero stress and particle velocity of magnitude u_2 for the configuration Fig. 2(a) [see Fig. 3(a)]. The corresponding release state attained at the target–window interface for the configuration Fig. 2(b) is stress (σ_3) and particle velocity (u_3). These two release waves, propagating towards each other interact at some depth in the target generating tensile stress waves (T_+ and T_-) in it at time t_4 [Fig. 2 (c)]. If the tensile stress generated exceeds the tensile strength (σ_T) of the material, then a free surface [shown by a vertical dashed line in Fig. 2 (c)] is generated in the region of this interaction in the target. Fig. 3(a) represents the two tensile waves T_+ and T_- by segments $u_2 - \sigma_T$ and $u_8 - \sigma_T$, respectively for Fig. 2(a). The corresponding tensile waves for Fig. 2(b) are represented by $\sigma_3 - u_{3'} - \sigma_T$ and $\sigma_4 - u_{4'} - \sigma_T$, respectively in Fig. 3(a). Implicit in this statement, is that the impedance of the window is very close, but distinctly different, from that of the free surface and as a consequence will not significantly influence the calculated value of the tensile impedance of the materials, even though the segments $\sigma_3 - u_{3'}$ and $\sigma_4 - u_{4'}$ transverse the compressive stress region. The generation of a free surface in the spalled target, results in a shock wave propagating back toward the free surface of the target or the target–window interface. This shock wave is represented by $\sigma_T - u_9$ for the configuration Fig. 2(a) in Fig. 3(a). And it is represented by $\sigma_T - u_{5'}$ for the second configuration in Fig. 3(a). Subsequent interactions are not relevant for the purpose of this new experiment. If, on the other hand, the tensile stress generated is smaller than the tensile strength of the material, then tensile stress waves of magnitudes σ_{T2} and σ_{T1} propagate for configurations (a) and (b), respectively, toward the impact surface of the target and the free surface of the target and the target–window interface. In either case target and impactor separate at time t_5, because, a tensile wave can not be transmitted through a material discontinuity.

If the material spalls at σ_T [Fig. 3(a)], the chronological excursions of recorded particle velocity at the free surface of the target due to the above described wave propagations and their interactions are u_2, u_8, and u_9. Similarly, the chronological excursion of the corresponding stress–particle velocity excursions monitored at the target-window (PMMA) interface due to the above described wave propagations and their interactions are (σ_3, u_3), (σ_4, u_4), and (σ_5, u_5). If the material does not spall, then the tensile stresses σ_{T1} and σ_{T2} are generated in such a simultaneous experiment [Fig. 3(b)]. The chronological excursions of particle velocity at the free surface are u_2 and $u_{8'}$ and the chronological excursions of stress and particle velocity at the target-window (PMMA) interface are (σ_3, u_3), and ($\sigma_{6'}$, $u_{6'}$).

Assuming that (i) the material spalls at σ_T, (ii) the effective tensile paths are linear, (iii) the Hugoniot, release, and re-shock behaviors of the window material are known, and (iv) the magnitudes of ($u_2 - u_8$) and ($u_{3'} - u_{4'}$) are the same, the spall stress (σ_T) is given by

$$\sigma_T = -0.5Z_T(u_2 - u_8) = -0.5Z_T(u_{3'} - u_{4'}). \tag{1}$$

And the spall stress is given by

$$\sigma_T = Z_T u_T + \sigma_3 - Z_T u_3, \text{ along } \sigma_3 - \sigma_T \text{ and} \tag{2}$$

$$\sigma_T = -Z_T u_T + \sigma_4 + Z_T u_4, \text{ along } \sigma_4 - \sigma_T. \tag{3}$$

Eqs. (1), (2), and (3) yield

$$Z_T = (\sigma_3 + \sigma_4)/(u_8 - u_2 + u_3 - u_4) \text{ and,} \tag{4}$$

$$\sigma_T = -0.5(\sigma_3 + \sigma_4)(u_2 - u_8)/(u_8 - u_2 + u_3 - u_4). \tag{5}$$

Thus, Eqs. (4) and (5) provide the magnitudes of effective tensile impedance and spall threshold for the material from the values of stress and particle velocities measured during the performance of the simultaneous experiment previously described. PMMA was used as the window material in this work for its low impedance and transparency. The Hugoniot of this material is well known and reported by Barker and Hollenbach (1970) and McQueen et al. (1970). In addition, its shock–release–reshock response was reported by Dandekar et al. (1988).

Shock wave experiments were performed on right circular disks of 93W. The diameters of the disks were 31.5 ± 1 mm. The disk thicknesses varied between 3 and 9 mm. The specimens were flat to 5 μm and the opposing faces were mutually parallel to better than 2 parts in 10^{-4} over the entire lateral dimension of the specimens. Materials used as an impactor in these experiments were Z-cut sapphire (Al_2O_3), copper (OFHC), x-cut quartz, and 93W. Stress in 93W was measured by an x-cut quartz gage. The particle velocities were measured by a four-beam velocity interferometer system for any reflector (four-beam VISAR). The precision of stress measurements by means of x-cut quartz gage is 3%. The precision of particle velocity measurements by means of the VISAR is estimated to be 1%. The planarity of the impact was better than 0.5 mrad. The impact velocities in these experiments were measured within an uncertainty of 0.5%.

4. Results

A summary of the results obtained from the plane shock wave transmission experiments is given in Table 2. Representative transmission wave profiles recorded in 93W are shown in Fig. 4.

4.1. Elastic compression

It is seen from Fig. 4 that the elastic precursor in this alloy, unlike in a single component ductile material, is sometimes dispersive even when the rise time does not exceed 20 ns. Whenever a well-defined cusp corresponding to the Hugoniot elastic limit (HEL) is missing in the wave profile, the value of particle velocity at which a break in the initial dispersivity of loading occurs, is taken to be at HEL. The average value of HEL obtained from these experiments is 2.76 ± 0.26 GPa. The large uncertainty in the value of the HEL is partly due to the difficulty in identification of

Table 2
Summary of shock experiments on 93W

Experiment		Thickness			Elastic			Plastic			
Number	Impactor/ window	Impactor (mm)	Target (mm)	Impact velocity (km/s)	Particle velocity (km/s)	Stress (GPa)	Density (mg/m^3)	Shock velocity[a] (km/s)	Stress (GPa)	Particle velocity (km/s)	Density (mg/m^3)
501-1	Al_2O_3/None	1.955	2.004	0.2488	0.0340	3.12	17.86	4.19	7.16	0.088	18.10
501-2	Al_2O_3/PMMA	1.953	2.001	0.2488	0.0315	2.89	17.86	4.14	7.12	0.089	18.10
446-1	93W/None	3.903	8.994	0.5116	0.0336	3.09	17.86	4.33	20.28	0.2558	18.83
446-2	93W/None	1.985	3.000	0.5116	0.0330	3.03	17.86	4.30	20.13	0.2558	18.84
324	93W/PMMA	2.992	5.971	0.6045	0.0277	2.55	17.84	4.32	23.71	0.3022	19.05
320-1	93W/None	2.978	6.106	0.4105	0.0275	2.53	17.84	4.21	15.89	0.2052	18.63
320-2	93W/PMMA	2.976	6.111	0.4105	0.0275	2.53	17.84	4.20	15.86	0.2052	18.63
316-1	93W/None	2.969	6.113	0.2478	0.0313	2.87	17.85	4.20	9.82	0.1239	18.26
316-2	93W/PMMA	2.981	6.112	0.2478	0.0300	2.76	17.85	4.18	9.77	0.1239	18.26
311-2	93W/PMMA	2.970	5.953	0.2473	0.0265	2.44	17.84	4.20	9.51	0.1237	18.27
305-2	Al_2O_3/PMMA	2.999	2.997	0.2079	0.0265	2.43	17.84	3.98	5.93	0.0747	18.05
305-3	Quartz/Quartz	4.315	2.390	0.2079	0.0284	2.72[b]	17.84				
220	OFHC/PMMA	3.134	6.092	0.3143	0.0260	2.390	17.84	4.10	8.03	0.1030	18.18

[a] Effective velocity in elastically deformed 93W.
[b] Stress recorded by a x-cut quartz gage.

the particle velocity at which a break in the initial dispersive rate of loading is observed. The precision of such a measurement for a nondispersive elastic precursor, based on the uncertainties in the measurements of density, longitudinal wave velocity, and particle velocity is estimated to be 1.4%. The error associated with the values of density at the HEL is 4% . Elastic precursors in polycrystalline tungsten (Asay et al., 1980) and in an annealed tungsten alloy of a similar composition alloy such as 93W (Baoping et al., 1994) showed similar dispersions. Baoping et al. (1994) found that the free surface velocities corresponding to HEL decreased from 0.072 km/s in a specimen of thickness 1.88 mm to 0.044 km/s in a specimen of thickness 11.68 mm. The present work does not show any evidence of an attenuation of the elastic precursor in 93W. For example, in experiments 446-1 and 446-2 conducted simultaneously on two specimens with thickneses 8.99 and 3.00 mm, the values of HEL are 3.09 and 3.03 GPa, respectively. These magnitudes of HEL correspond to 0.067 and 0.066 km/s as the free surface velocity for 93W.

4.2. Inelastic compression

The magnitude of the shock velocity, following the elastic precursor, lie between 3.98 and 4.33 km/s (Table 2). It tends to increase with an increase in the value of the peak stress. These values are comparable to the value of bulk sound speed 4.04 ± 0.10 km/s in 93W calculated from the longitudinal and shear elastic wave velocities for this alloy given in Table 1. This implies that 93W retains its shear strength above the HEL (Graham and Brooks, 1971), and, as such, this alloy deforms plastically above its HEL. This information is used to calculate the free surface velocities or the particle velocities at the alloy–PMMA window interface to

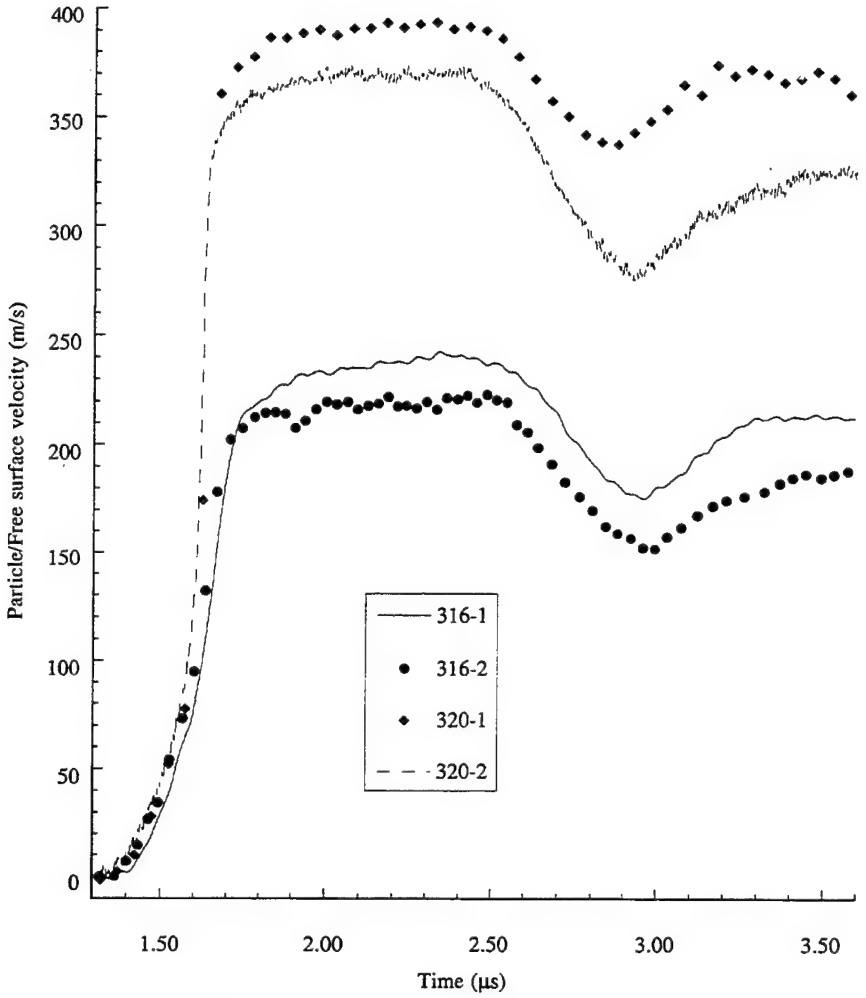

Fig. 4. Representative particle/free surface velocity profiles in 93W.

validate the inference about the plastic deformation of the tungsten alloy above its HEL. The calculated values of the free surface velocities and the particle velocities at the alloy–PMMA window interface are compared with their respective measured values in Table 3. This table shows that the calculated values of the particle velocities and their measured values are within 4.5% for all transmission experiments (e.g. within the error of measurements). This supports the inference that the inelastic deformation of 93W under compression and release proceeds in the manner of an elastic–plastic solid. A direct impact experiment was conducted to obtain values of stress (σ)-particle velocity (u) coordinates under shock compressed and release states at the impact surface of a 93W specimen. In this experiment a specimen of 93W impacted a 1 mm thick tungsten carbide disk bonded to a x-cut quartz gage with a velocity of 0.247 km/s. The Hugoniot of the tungsten carbide reported by Karnes (1972 unpublished) was used to analyze the stress data recorded by the quartz gage. The results of this experiment yielded the shock and release (σ, u) coordinates as (10.77, 0.1360), and (3.68, 0.0513), respectively. Stress and particle velocity are in the units of GPa and km/s, respectively. These coordinates are consistent with the

Table 3
Measured and calculated particle velocities in transmission experiments on 93W tungsten alloy

Experiment	Particle velocity (km/s)		Difference %
	Measured	Calculated	
501-1	0.166	0.169	1.8
501-2[a]	0.164	0.162	1.2
446-1	0.5105	0.5052	1.0
446-2	0.5012	0.5050	0.7
324[a]	0.5454	0.5696	4.4
320-1	0.3946	0.4040	2.4
320-2[a]	0.3693	0.3840	4.0
316-1	0.2304	0.2407	4.0
316-2[a]	0.2234	0.2295	2.7
311-2[a]	0.2209	0.2299	4.0
305-2[a]	0.1292	0.1340	3.8
220[a]	0.1846	0.1899	2.8

[a] Particle velocity at the tungsten alloy–PMMA interface.

compression (Fig. 5) and release behavior of 93W as measured by its release impedance obtained from transmission experiments (Table 4).

Since the deformation of 93W above its HEL proceeds plastically, an estimate can be made of the magnitude of shear stress sustained by the alloy and associated longitudinal plastic strain induced in it as a function of impact stress. Such an estimation can be done in three ways (Asay et al., 1980): (i) by comparison of longitudinal stress states with hydrostatic response, (ii) by differential relation for shear stress, and (iii) by self-consistent determination of shear stress. Since neither the hydrostatic response nor experimental results pertaining to the third method are available for 93W at the present time, the second method of the estimation is adopted for calculating the magnitude of shear stress and strain under shock compression. This method uses the observed wave profiles to calculate shear stress and plastic strain by using the differential relation between longitudinal stress and total strain. This method depends on determining density states (ρ) i.e. total strain (e) in the material from in situ stress (σ) histories (Fowles and Williams, 1970) given by

$$de = d\sigma/\rho_o C^2, \text{ and} \tag{6}$$

$$e = 1 - (\rho_o/\rho), \tag{7}$$

where are ρ_o, and ρ are the initial, and final densities, respectively, and C is the Lagrangian wave velocity corresponding to a stress increment in the profile.

And by using the relationship (Fowles, 1961) between the impact stress $[\sigma(e)]$, shear stress $[\tau(e)]$, and hydrodynamic pressure $[P(e)]$ at a given strain (e), namely,

$$\tau(e) = 0.75[\sigma(e) - P(e)]. \tag{8}$$

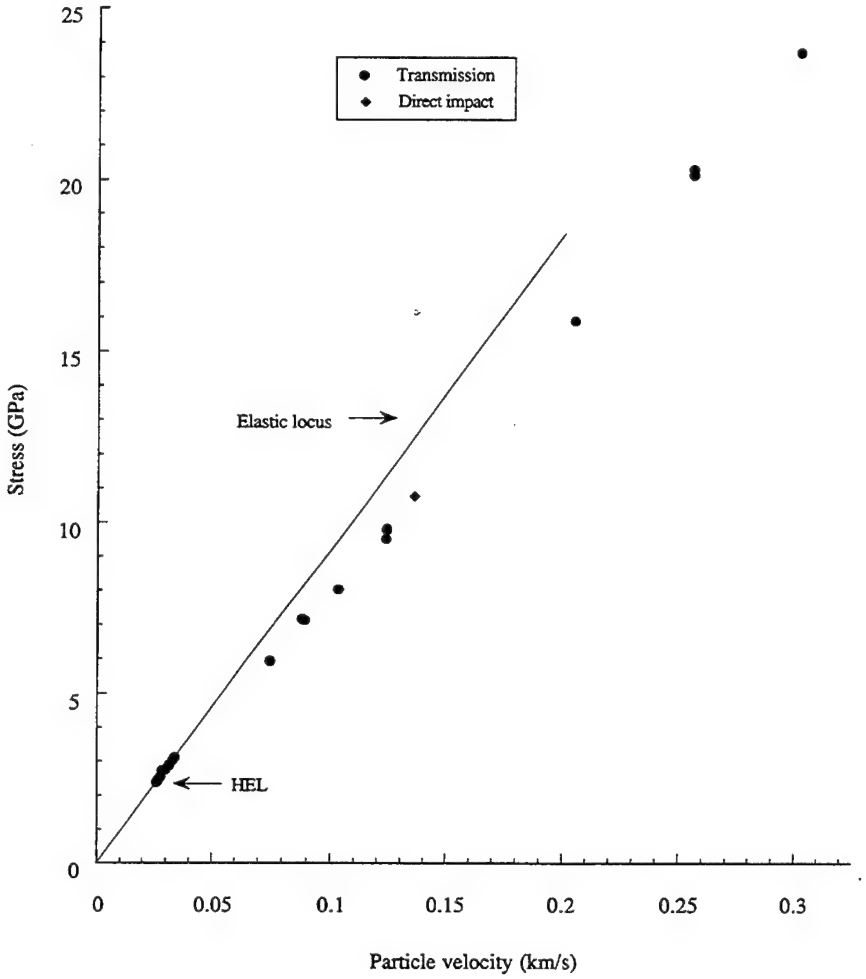

Fig. 5. Stress–particle velocity diagram for 93W.

Table 4
Release wave velocities and release wave impedance of 93W alloy

Experiment	Leading edge release wave velocity (km/s)	Release impedance Gg/m^2s
501-1	5.25	82
501-2	5.25	83
446-2	5.37	80
324	5.56	88
320-1	5.30	80
320-2	5.30	88
316-1	5.10	84
316-2	5.10	90
311-2	5.21	89
305-2	5.32	100
220	—	94

The differential equation for shear stress given by Eq. (6) can be expressed in the following form (Fowles, 1961)

$$(d\tau/de) = (\rho/\rho_o)\mu - 0.75\rho_o[C_L^2 - C^2] \tag{9}$$

by using Eqs. (7) and (8).

In relation (9), C_L is the Lagrangian longitudinal elastic wave velocity at a given strain, and μ is the shear modulus. The accuracy of the calculated value of the shear stress as a function of strain depends on the knowledge of C_L and μ of the material at a given strain state during shock loading or unloading. The estimates of C_L obtained from the transmission wave profiles are given in Table 4. Since the value of shear modulus of 93W is not presently available as a function of pressure or strain its value at the ambient condition is substituted in Eq. 9 to calculate values of the shear stresses given in Table 5. These values underestimate the shear stress if the strain derivative of the shear modulus is positive.

The plastic i.e. strain (e_p) in terms of total strain, can be calculated from the differential relation (Fowles, 1961),

$$de_p = 2/3[de - d\tau/\mu]. \tag{10}$$

The calculated values of shear stress and plastic strain along with the longitudinal/impact stress and total strain generated in 93W are given in Table 5. This table shows that the shear stress sustained by 93W increases with an increase in the impact stress. The results obtained for experiments 305-2 and 220 appear inconsistent with those of other 10 experiments. There is no explanation for these observed inconsistencies. However, replicability of the estimates of impact and shear stresses and total and plastic strains is quite good as seen from the results of simultaneous experiments 501, 446, 320 and 316. The magnitude of shear stress sustained in the compression-shear experiments conducted in 93W at normal impact stress between 9.6 and 10.5 GPa vary between 1.2 and 1.3 GPa (Zhou et al., 1992). Our experiments

Table 5
Calculated values of impact and shear stresses and total and plastic strains in 93W

Experiment	Impact stress (GPa)	Shear stress (GPa)	Total strain	Plastic strain
501-1	7.16	1.16	0.0195	0.0075
501-2	7.12	1.08	0.0195	0.0078
446-1	20.28	3.04	0.0575	0.0239
446-2	20.13	2.88	0.0580	0.0250
324	23.71	3.35	0.0674	0.0290
320-1	15.89	1.85	0.0474	0.0228
320-2	15.86	1.80	0.0474	0.0230
316-1	9.82	1.31	0.0281	0.0125
316-2	9.77	1.26	0.0281	0.0127
311-2	9.51	1.25	0.0281	0.0128
305-2	5.93	0.70	0.0168	0.0079
220	8.03	0.89	0.0238	0.0116

indicate the magnitude of shear stress sustained by this alloy at 9.7 GPa to be 1.3 GPa. This may indicate that the influence of the pressure dependence of μ is minimal to at least 10 GPa. However, these results need to be confirmed independently by carrying out shock re-shock experiments in 93W as done by Asay et al. (1980) or of the type reported by Dandekar et al. (1988) and Dandekar (1994) and/or by determining the hydrodynamic compression of 93W by conducting compression-shear experiments.

4.3. Release characteristic

The character of initial release of the shock compressed state due to arrival of rarefaction from the free surface of the specimens can be discerned through calculations of release impedance from: (i) the value of release wave velocity derived from the pulse width of the shock compression pulse and the density at the peak compressive stress and (ii) the measured values of the peak stress and release stress and respective particle velocities. The measured value of release stress at the specimen–PMMA interface is obtained from the Hugoniot of PMMA. The values of leading edge release stress wave velocities and the values of impedance calculated in the aforementioned manner are given in Table 4. In this table, a totally stress free state in an experiment occurs when the alloy specimen in that experiment was not bonded to a PMMA disk. The magnitudes of release wave velocities are very close to the longitudinal wave velocity, indicating that the initial release in this alloy is attained elastically.

4.4. Tensile impedance and spall threshold

The tensile impedance of 93W was obtained by conducting the new experiment described in Section 3. The results of three experiments conducted to obtain the value of tensile impedance of 93W are given in Table 6. Based on the shock and release response of the alloy, the peak values of impact stresses were selected so that tensile stress due to the interaction of release waves propagating in the 93W target would be generated through plastic deformation. Experimental difficulties prevented the carrying out of an experiment where the tensile condition in 93W would have been attained through elastic release completely. The values of tensile impedance of 93W when preshocked between 7 and 20 GPa vary from 64 and 76 Gg/m^2 s. Dandekar

Table 6
Measured values of free surface velocities, particle velocities at the specimen–PMMA interface, and values of tensile impedance of 93W at various peak stresses

Experiment	u_2 (km/s)	u_8 (km/s)	u_3 (km/s)	u_4 (km/s)	Tensile impedance (Gg/m^2 s)	Peak stress (GPa)
501	0.166	0.113	0.1635	0.096	64.9	7.14
320	0.395	0.3399	0.369	0.276	64.1	15.87
316	0.230	0.175	0.223	0.150	76.2	9.80

and Weisgerber (1998) showed that with 1% error in the measurement of particle velocity by means of VISAR, the uncertainty in the values of the tensile impedance is ± 10 Gg/m^2 s. These values are close to the bulk impedance 71.7 ± 1.8 Gg/m^2 s of 93W. In other words, these values suggest that the tensile stress states in 93W were generated following the expected plastic deformation history.

The values of spall threshold of 93W are given in Table 7, both as a function of compressive pulse width and impact stress. It is worth noting that the observed magnitudes of pull-back particle velocities, irrespective of pulse width and impact stress are around 0.05 km/s. This implies that the spall strength of 93W as measured by pull-back particle velocity is invariant based on the limited number of experiments performed in this work. Considering this and the fact that errors of measurement associated with the values of tensile impedance, it is reasonable to convert the pull-back particle velocities by multiplying half their value with an average value of the tensile impedance to calculate the values of spall threshold in terms of stress (Table 7). The value of spall threshold varies between 1.7 and 2 GPa, less than the magnitude of its HEL (i.e. 2.8 GPa). In this regard 93W differs from other ductile metallic materials and alloys in that their spall threshold values exceed their HEL.

5. Shock response of 93W, 90W, W-2, and polycrystalline tungsten

5.1. Elastic deformation

Deformation behavior of 93W, 93W(A), 90W, W-2, and polycrystalline tungsten (W) under plane shock wave propagation is summarized in Table 8. It should be noted that the ratio of Ni and Fe in these alloys is 7:3, even though actual weight percentage of these elements differs in these three tungsten alloys. Further these materials are composites rather than well defined alloys because they consist of two phases, namely, a nearly spherical grains of body-centered-cubic tungsten phase surrounded by a face-centered-cubic matrix phase composed of W, Ni, and Fe or, W, Ni, Fe, Cu, and Co. The composition of the matrix phase is dependent upon the ratio of Ni to Fe in these alloys. The Hugoniot of the matrix phase remains unavailable.

Table 7
Spall threshold of 93W

Experiment	Pulse width (μs)	Impact stress (GPa)	Pull back particle velocity (km/s)	Spall threshold (GPa)
501	0.35	7.14	0.053	1.8
446-2	0.766	20.1	0.056	1.9
324	1.15	23.71	–	2.0
320	1.15	15.87	0.057	2.0
316	1.15	9.80	0.055	1.9
311-2	1.15	9.51	–	2.0
305-2	0.54	5.93	–	2.0
220	1.40	8.03	0.051	1.7

Without the expected values of HEL or volumetric compression of these alloys to examine validity of any specific model for composites the only possible observation that can be made under the circumstance is that the HEL of polycrystalline tungsten is lowered when it is alloyed but does not appear to be correlated progressively with either the amount of tungsten phase or the amount of the matrix phase. For example, whereas, the HEL of 93W is found to be 2.76 ± 0.26 the HEL of 90W is reported to be 1.5 ± 0.4 GPa by Hauver (1980) and 2.62–3.1 GPa by Chang and Choi (1998), respectively. The HEL of polycrystalline W is 3.6 ± 0.1 GPa (Asay et. al., 1980). Additionally, the HEL of swaged or annealed 93W do not seem to differ significantly from one another (Table 8).

5.2. *Inelastic response and volumetric compression*

Rabin and German (1988) showed that increasing tungsten content in W composites results in strengthening and drastic decrease in the ductility of the alloy. Two measures of ductility of a material under plane shock loading are magnitudes of shear stress sustained under shock compression and spall threshold under shock induced tension. The results presented in this work tends to bear out the observations of Rabin and German (1988) but not completely. The magnitude of shear stress sustained in polycrystalline W (Asay et al., 1980) and 93W when shocked to 9.7 GPa are 0.8 and 1.3 GPa, respectively (Table 8). However, the shear stress sustained in W2 is only 0.5 GPa. The data reported by Baoping et al. (1994) on 93W(A) does not permit calculation of the shear stress sustained by the alloy under shock wave propagation. The same holds true for the data reported for 90W by Hauver (1980) and Chang and Choi (1998).

The volumetric compressions of these alloys and polycrystalline tungsten under shock are shown in Fig. 6. The qualitative aspect of this figure shows that tungsten alloys are more compressible than the unalloyed tungsten. The volumetric compression of 90W reported by Hauver (1980) and Chang and Choi (1998) are consistent with one another. These results indicate that alloying tungsten with an increasing amount of nickel and iron makes it relatively more compressible. Lack of the Hugoniot data for the matrix phase of these tungsten alloys prohibits calculations of the compressibility curves for them. Any generalization based on the

Table 8
Summary of deformation behaviors of polycrystalline tungsten (W), 93W, 93W(A), 90W, and W-2

	Units	W Asay et al. (1980)	93W	93W (A) Baoping et al. (1994)	90W Hauver (1980)	90W Chang and Choi (1998)	W-2 Gaeta and Dandekar (1988)
HEL	GPa	3.6 ± 0.1	2.76 ± 0.26	2.0–3.3	1.5 ± 0.4	2.62	2.02–1.15
Deformation above the HEL		Some loss of shear strength	Elastic–plastic	Not reported	Elastic–plastic	Not reported	Elastic–plastic
Shear stress at impact stress 10 GPa	GPa	0.8	1.27 ± 0.06	Not reported	Not reported	Not reported	0.5
Spall threshold	GPa	0.42–0.66	1.8–2.1	0.54–3.04	No data	3.7–5.6	No data

observed shock compressions of metals and their alloys are not applicable to the compression behaviors of these W alloys because of their composite nature.

5.3. Spall strength

The spall strengths of polycrystalline W (Asay et al., 1980) and 93W are 0.4–0.6 and 1.9 ± 0.4 GPa, respectively. Zurek and Gray (1991) reported spall strength of 0.4 GPa for polycrystalline W(recrystallized) and 0.8 GPa for cold rolled W. Baoping et al. (1994) report that spall strength of 93W(A) increases from 0.54 to 3 GPa when it is increasingly shocked between 21 and 30 GPa. Subjected to a further increase in the stress its spall strength decreases to 1.56 GPa at 32 GPa. The present data on 93W does not show any change in the value of its spall strength when subjected to a stress between 5.9 and 24 GPa. Similarly, Chang and Choi (1998) report that the spall strength of 90W increases from 3.74 to 5.6 GPa when subjected to increasing impact stress from 5.52 to 23 GPa. Zurek and Gray (1991) reported the spall strength of 90W-7Ni-3Fe to be 3.4–3.8 GPa when shocked to 15 GPa. Thus under tension alloyed tungsten exhibits more ductility than unalloyed polycrystalline W.

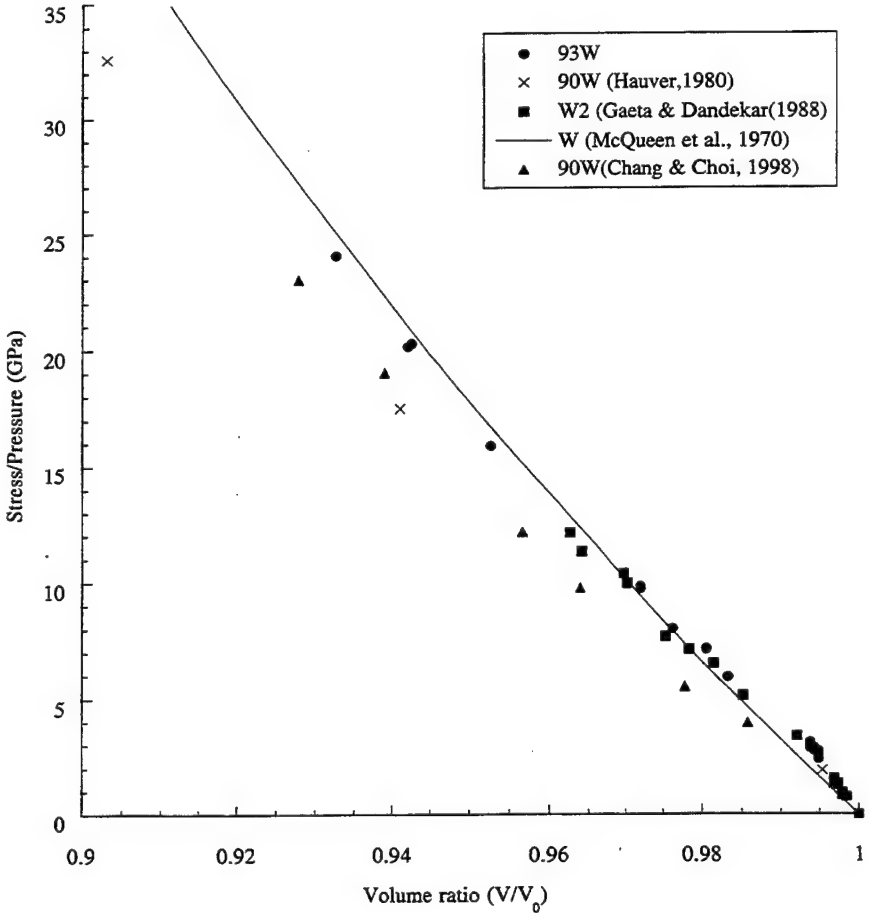

Fig. 6. Compression of tungsten and its alloys.

And in the case of 90W, its spall strength is actually higher than the value of its HEL as in other ductile metals and alloys. However, the spall strength of 93W is lower than its HEL (Table 8). No spall data are available for W-2 to compare with these results. One possible reason for the observed trend in the spall strengths of tungsten and its alloys may be as follows. The poor ductility of polycrystalline tungsten is reflected by its high HEL, progressively lower magnitude of shear stress sustained under shock compression i.e. resistance to plastic flow. Physical implication of a loss of shear strength under plane shock wave loading in metallic material remains unclear. However, if the flow stress level in polycrystalline W exceeds the grain boundary fracture stress it could lead to intergranular fracture which may lead to a low spall threshold value (Zurek and Gray, 1991). Zurek and Gray (1991) showed that whereas fracture morphology of the recovered W (recrystallized) is intergranualar the morphology of cold rolled W is due to cleavage. The weakest link in tungsten alloyed with Ni, Fe, and other elements is W–W interface so that the fracture of W–W interface is relatively easier than of a W grain. Thus, ductility of the matrix phase (M) and the bond strength of W–M interface dictates the ductility of the alloy. Baoping et. al. (1994) reported that recovered annealed 93W when shocked between 21 and 32 GPa show: (i) no change in the area of W–W interface separation (20%) with shock stress, (ii) W–M interface separation had a minima around 30 GPa, and (iii) the remaining fracture modes due to M–M separation and cleavage of W grains had maximum at 30 GPa. Baoping et. al. (1994) thus surmised that the annealed 93W retained significant ductility to 30 GPa above which it became brittle, and thus providing explanation for the observed increase in the spall strength of the annealed 93W from 0.54 to 3.04 GPa when shocked between 21 and 30 GPa, and the reduction of its spall strength to 1.56 GPa when shocked to 32 GPa. Further, they attributed the onset of brittleness in the annealed 93W to formation of a new phase of composition 75W-15Ni-10Fe at the W–M interface at 32 and higher GPa. In the present work, we were unable to recover any material for post shock examination. Hence, we cannot confirm whether the above explanation also holds for swaged 93 W used in the present work. But if we restrict our attention to the shock response of the both the annealed and swaged 93W to 24 GPa, the spall threshold values of the swaged and the annealed material are 1.9 ± 0.4 GPa, and less than 1 GPa, respectively. These values are less than the respective HELs of these two 93W. Thus, it is difficult to provide a satisfactory explanation for the observed low spall strength of 93W in spite of the observed ductility under shock compression without performing shock wave experiments on the matrix phase material and examination of shock recovered matrix phase material and 93W.

6. Summary

The shock response of polycrystalline tungsten and its alloys may be summarized as follows:

1. Hugoniot elastic limits of tungsten are lowered through alloying it with nickel and iron.

2. Alloying tungsten makes it ductile under shock compression, and as, a consequence, it sustains larger shear stress than the pure polycrystalline tungsten.
3. Another consequence of ductility of a tungsten alloy is manifested by an increase in spall threshold of the alloy compared to the pure polycrystalline tungsten.
4. Volumetric compression of tungsten alloys tends to increase at a given stress as the weight percentage of tungsten in the alloy is decreased.

References

Asay, J.R., Chhabildas, L.C., Dandekar, D.P., 1980. Shear strength of shock-loaded polycrystalline tungsten. J. Appl. Phys 51, 4774–4783.

Baoping, Z., Chao, Y., Yingming, X., Chunlan, J., 1994. Responsive behavior of 93 wt.% tungsten alloy under the intense shock loading. In: Zhemin, Z., Quingming, T. (Eds.), Proceedings of IUTAM Symposium on Impact Dynamics. Peking University Press, Peking, PRC, pp. 283–297.

Barker, L.M., Hollenbach, R.E., 1970. Shock-wave studies of PMMA, fused silica, and sapphire. J. Appl. Phys 41, 4208–4226.

Chang, S.N., Choi, J.H., 1998. High strain rate response of a tungsten heavy alloy. In: Schmidt, S.C., Dandekar, D.P., Forbes, J.W. (Eds.), Shock Compression of Condensed Matter — 1997. American Institute of Physics, Woodbury, New York, pp. 415–418.

Dandekar, D.P., 1976. Loss of shear strength in polycrystalline tungsten under shock compression. J. Appl. Phys 47, 4703–4705.

Dandekar, D.P., 1994. Response of protective ceramics under single and multiple impacts. In: Kinara, V.K., Clifton, R.J., Johnson, G.C. (Eds.), Wave Propagation and Emerging Technologies, AMD-Vol. 188. ASME Press, New York, pp. 133–141.

Dandekar, D.P., 1996. Experimental technique to measure tensile impedance of a material under plane shock wave propagation. In: Schmidt, S.C., Tao, W.C. (Eds.), Shock Compression of Condensed Matter — 1995. American Institute of Physics, Woodbury, New York, pp. 947–950.

Dandekar, D.P., Gaeta, P.J., Horie, Y., 1998. Double shock and release experiments in PMMA and z-cut sapphire. In: Schmidt, S.C., Holms, N.C. (Eds.), Shock Compression of Condensed Matter — 1987. North-Holland, Amsterdam, pp. 281–284.

Dandekar, D.P., Weisgerber, W., 1998. Shock induced deformation of tungsten and one of its alloys. In: Shim, V.P.W., Tanimura, S., Lim, C.T. (Eds.), Impact Response of Materials and Structures. Oxford, Singapore, pp. 235–240.

Ekbom, L., 1981. Microstructural study of the deformation and fracture behavior of a sintered tungsten-base composite. In: Hausner, H.H., Antes, H.W., Smith, G.D. (Eds.), Modern Developments in Powder Metallurgy 14. Metal Powder Industries Federation, Princeton, pp. 177–188.

Fowles, G.R., 1961. Shock wave compression of hardened and annealed 2024 aluminum. J. Appl. Phys. 32, 1475–1487.

Fowles, G.R., Williams, R.F., 1970. Plane stress wave propagation in solids. J. Appl. Phys. 41, 360–363.

Gaeta, P.J., Dandekar, D.P., 1988. Shock response of Kennertium grade W-2. In: Schmidt, S.C., Holms, H.C. (Eds.), Shock Waves in Condensed Matter-1987. Elsevier, New York, pp. 269–272.

Graham, R.A., Brooks, W.P., 1971. Shock-wave compression of sapphire from 15 to 420 kbar. The effects of large anisotropic compressions. J. Phys. Chem. Solids 32, 2311–2330.

Hauver, G.E., 1980. The Hugoniot for 90 W-7 Ni-3Fe tungsten alloy, ARBRL-MR-02987, U. S. Army Ballistic Research Laboratory Report, Aberdeen Proving Ground, Maryland.

Hofmann, H., Petzow, G., 1984. Influence of sintering atmosphere on mechanical properties of tungsten based heavy alloys. In: Hausner, H.H., Antes, H.W., Smith, G.D. (Eds.), Developments in Powder Metallurgy 17. Metal Powder Industries Federation, Princeton, pp. 17–31.

Lowrie, R., Gonas, A.M., 1965. Single -crystal elastic properties of tungsten from 24 to 1800 C. J. Appl. Phys 38, 4505–4509.

McQueen, R.G., Marsh, S.P., Taylor, J.W., Fritz, J.N., Carter, W.J., 1970. The equation of state of solids from shock wave studies. In: Kinslow, R. (Ed.), High Velocity Impact Phenomena. Academic, New York, pp. 293–417.

O'Donnell, R.G., Woodward, R.L., 1990. The composition and temperature dependence of the mechanical properties of tungsten alloys. Met. Transc. A 21A, 744–748.

Rabin, H.B., German, R.M., 1988. Microstructure effects on tensile properties of tungsten-nickel-iron composites. Met. Trans. A 19A, 1523–1532.

Weerasooriya, T., Moy, P., 1998. High shear strain-rate behavior of W–Ni–Fe tungsten heavy alloy composites as a function of matrix volume fraction. ARL-TR-1694, U. S. Army Research Laboratory, Aberdeen Proving Ground, Maryland.

Zhou, M., Clifton, R. J. & Needleman, A., 1992. Shear band formation in a W–Ni–Fe alloy under plate impact. In: Proceedings of 1992 International Conference on Tungsten and tungsten Alloys. Metal powder Federation, Princeton, pp. 343–356.

Zurek, A.K., Gray III, G.T., 1991. Dynamic strength and strain rate effects on fracture behavior of tungsten and tungsten alloys. J. De Physique IV Colloque C3, 631–637.

INTENTIONALLY LEFT BLANK.

NO. OF COPIES	ORGANIZATION
2	DEFENSE TECHNICAL INFORMATION CENTER DTIC DDA 8725 JOHN J KINGMAN RD STE 0944 FT BELVOIR VA 22060-6218
1	HQDA DAMO FDT 400 ARMY PENTAGON WASHINGTON DC 20310-0460
1	OSD OUSD(A&T)/ODDDR&E(R) R J TREW THE PENTAGON WASHINGTON DC 20301-7100
1	DPTY CG FOR RDA US ARMY MATERIEL CMD AMCRDA 5001 EISENHOWER AVE ALEXANDRIA VA 22333-0001
1	INST FOR ADVNCD TCHNLGY THE UNIV OF TEXAS AT AUSTIN PO BOX 202797 AUSTIN TX 78720-2797
1	DARPA B KASPAR 3701 N FAIRFAX DR ARLINGTON VA 22203-1714
1	US MILITARY ACADEMY MATH SCI CTR OF EXCELLENCE MADN MATH MAJ HUBER THAYER HALL WEST POINT NY 10996-1786
1	DIRECTOR US ARMY RESEARCH LAB AMSRL D D R SMITH 2800 POWDER MILL RD ADELPHI MD 20783-1197

NO. OF COPIES	ORGANIZATION
1	DIRECTOR US ARMY RESEARCH LAB AMSRL DD 2800 POWDER MILL RD ADELPHI MD 20783-1197
1	DIRECTOR US ARMY RESEARCH LAB AMSRL CI AI R (RECORDS MGMT) 2800 POWDER MILL RD ADELPHI MD 20783-1145
3	DIRECTOR US ARMY RESEARCH LAB AMSRL CI LL 2800 POWDER MILL RD ADELPHI MD 20783-1145
1	DIRECTOR US ARMY RESEARCH LAB AMSRL CI AP 2800 POWDER MILL RD ADELPHI MD 20783-1197
	ABERDEEN PROVING GROUND
4	DIR USARL AMSRL CI LP (BLDG 305)

NO. OF COPIES	ORGANIZATION
1	COMMANDER US ARMY ARDEC G FLEMING PICATINNY ARSENAL NJ 07806-5000
2	COMMANDER US ARMY ARDEC AMSTA AR FSA E E BAKER D KAPOOR PICATINNY ARSENAL NJ 07806-5000
2	SOUTHWEST RSRCH INSTITUTE C ANDERSON J LANKFORD PO DRAWER 28510 SAN ANTONIO TX 78228-0510
1	DIRECTOR LOS ALAMOS NATIONAL LAB MS B296 G T GRAY PO BOX 1663 LOS ALAMOS NM 87545
1	AIR FORCE WRIGHT LAB TECH LIB J FOSTER ARMAMENT DIVISION 101 EGLIN AVE STE 239 EGLIN AFB FL 32542
1	LOS ALAMOS NATIONAL LAB D RABERN GROUP MEE 13 MSJ576 LOS ALAMOS NM 87545
1	LOS ALAMOS NATIONAL LAB TECH LIB PO BOX 1663 LOS ALAMOS NM 87545
1	JOHNS HOPKINS UNIVERSITY DEPT MECH ENGINEERING K RAMESH CHARLES AND 33 ST BALTIMORE MD 21218

NO. OF COPIES	ORGANIZATION
1	PENN STATE UNIVERSITY COLLEGE OF ENGINEERING R GERMAN UNIVERSITY PARK PA 16802-6809
1	BROWN UNIVERSITY DIV OF ENGINEERING R CLIFTON PROVIDENCE RI 02912
1	UC SAN DIEGO DEPT APPL MECH AND ENG SVCS R011 S NEMAT NASSER LA JOLLA CA 92093-0411
1	CALTECH G RAVICHANDRAN MS 105 50 1201 E CALIFORNIA BLVD PASADENA CA 91125
1	INST OF ADVANCE TECH UNIV OF TX AUSTIN S J BLESS 4030 2 W BRAKER LN AUSTIN TX 78759
3	COMMANDER US ARMY RSRCH OFFC A CROWSON A RAJENDRAN D STEPP PO BOX 12211 RESEARCH TRIANGLE PARK NC 27709-2211
1	VIRGINIA POLYTECHNIC INST COLLEGE OF ENGNR R BATRA BLACKSBURG VA 24061-0219
1	DIR LLNL D LASILA L170 LIVERMORE CA 94550

NO. OF
COPIES ORGANIZATION

ABERDEEN PROVING GROUND

50 DIR USARL
AMSRL WM T
T WRIGHT
AMSRL WM TA
W GILLICH
W BRUCHEY
M BURKINS
P KINGMAN
J RUNYEON
W A GOOCH
AMSRL WM TC
T BJERKE
E KENNEDY
R MUDD
W WALTERS
L MAGNESS
R COATES
B SORENSON
D SCHEFFLER
K KIMSEY
AMSRL WM TD
A M DIETRICH
D DANDEKAR (15 CPS)
E RAPACKI
N RUPERT
T HADUCH
S SCHOENFELD
K FRANK
M RAFTENBERG
S SEGLETES
T WEERASOORIYA
AMSRL WM MA
P MOY
AMSRL WM MB
B FINK
C HOPPEL
G GAZONAS
AMSRL WM MC
R ADLER
M STAKER
E CHIN
AMSRL WM MD
W DEROSSET
R DOWDING
K CHO

INTENTIONALLY LEFT BLANK.

REPORT DOCUMENTATION PAGE

Form Approved
OMB No. 0704-0188

1. AGENCY USE ONLY *(Leave blank)*	2. REPORT DATE	3. REPORT TYPE AND DATES COVERED
	October 2000	Reprint, 16 November 1998

4. TITLE AND SUBTITLE
Shock Response of a Heavy Tungsten Alloy

5. FUNDING NUMBERS

6. AUTHOR(S)
Dattatraya P. Dandekar and William J. Weisgerber

7. PERFORMING ORGANIZATION NAME(S) AND ADDRESS(ES)
U.S. Army Research Laboratory
ATTN: AMSRL-WM-T
Aberdeen Proving Ground, MD 21005-5066

8. PERFORMING ORGANIZATION REPORT NUMBER
ARL-RP-9

9. SPONSORING/MONITORING AGENCY NAMES(S) AND ADDRESS(ES)

10.SPONSORING/MONITORING AGENCY REPORT NUMBER

11. SUPPLEMENTARY NOTES
A reprint from the *International Journal of Plasticity*, vol. 15, pp. 1291–1309, August 1999.

12a. DISTRIBUTION/AVAILABILITY STATEMENT
Approved for public release; distribution is unlimited.

12b. DISTRIBUTION CODE

13. ABSTRACT *(Maximum 200 words)*

This article describes the results of shock wave experiments performed on a heavy tungsten alloy containing W, Ni, and Fe in the ratio of 92.85:4.9:2.25 by weight. These experiments provide information about the shear strength under compression and tensile strength, as measured by the spall threshold, of this alloy to 24 GPa. The results of these experiments show that: (i) the magnitude of its Hugoniot elastic limit (HEL) is 2.76 ± 0.26 GPa; (ii) this alloy deforms plastically above its HEL and thus retains its shear strength to 24 GPa; (iii) the spall strength of the alloy is found to be 1.9 ± 0.4 GPa and is independent of the impact stress and duration of the shock compression pulse; and (iv) the tensile impedance of the alloy, determined from a new experiment designed to measure this impedance, is 68 ± 10 Gg/m^2 s.

14. SUBJECT TERMS	15. NUMBER OF PAGES
shock, tungsten, elastic-plastic	25
	16. PRICE CODE

17. SECURITY CLASSIFICATION OF REPORT	18. SECURITY CLASSIFICATION OF THIS PAGE	19. SECURITY CLASSIFICATION OF ABSTRACT	20. LIMITATION OF ABSTRACT
UNCLASSIFIED	UNCLASSIFIED	UNCLASSIFIED	UL

INTENTIONALLY LEFT BLANK.

USER EVALUATION SHEET/CHANGE OF ADDRESS

This Laboratory undertakes a continuing effort to improve the quality of the reports it publishes. Your comments/answers to the items/questions below will aid us in our efforts.

1. ARL Report Number/Author ARL-RP-9 (Dandekar) Date of Report October 2000

2. Date Report Received _____

3. Does this report satisfy a need? (Comment on purpose, related project, or other area of interest for which the report will be used.) _____

4. Specifically, how is the report being used? (Information source, design data, procedure, source of ideas, etc.) _____

5. Has the information in this report led to any quantitative savings as far as man-hours or dollars saved, operating costs avoided, or efficiencies achieved, etc? If so, please elaborate. _____

6. General Comments. What do you think should be changed to improve future reports? (Indicate changes to organization, technical content, format, etc.) _____

CURRENT ADDRESS

_____
Organization

_____
Name E-mail Name

_____
Street or P.O. Box No.

_____
City, State, Zip Code

7. If indicating a Change of Address or Address Correction, please provide the Current or Correct address above and the Old or Incorrect address below.

OLD ADDRESS

_____
Organization

_____
Name

_____
Street or P.O. Box No.

_____
City, State, Zip Code

(Remove this sheet, fold as indicated, tape closed, and mail.)
(DO NOT STAPLE)

DEPARTMENT OF THE ARMY

OFFICIAL BUSINESS

NO POSTAGE
NECESSARY
IF MAILED
IN THE
UNITED STATES

BUSINESS REPLY MAIL
FIRST CLASS PERMIT NO 0001,APG,MD

POSTAGE WILL BE PAID BY ADDRESSEE

DIRECTOR
US ARMY RESEARCH LABORATORY
ATTN AMSRL WM TD
ABERDEEN PROVING GROUND MD 21005-5066